energies

MDPI

Article

Evaluation of the Transient Overvoltages of HVDC Transmission Lines Caused by Lightning Strikes

Amr S. Zalhaf [1,2], Ensheng Zhao [1], Yang Han [1,*], Ping Yang [1], Abdulrazak H. Almaliki [3] and Reda M. H. Aly [3]

[1] School of Mechanical and Electrical Engineering, University of Electronic Science and Technology of China, Chengdu 611731, China; amr.zalhaf@uestc.edu.cn (A.S.Z.); zhaoens@163.com (E.Z.); ping@uestc.edu.cn (P.Y.)
[2] Electrical Power and Machines Engineering Department, Tanta University, Tanta 31511, Egypt
[3] Department of Civil Engineering, Faculty of Engineering, Taif University, Taif 21944, Saudi Arabia; a.almaliki@tu.edu.sa (A.H.A.); rmaly@tu.edu.sa (R.M.H.A.)
* Correspondence: hanyang@uestc.edu.cn

Abstract: High-voltage direct-current (HVDC) transmission systems are considered an outstanding solution due to high electrical losses emerging from long-distance transmission. However, HVDC transmission lines (TLs) are vulnerable to lightning strikes. In this work, the Yunnan-Guizhou 500 kV HVDC transmission system is used as a case study to evaluate the impact of lightning strikes on DC-TL overvoltages, as no research studies have been conducted to assess the lightning transient behavior of DC-TLs. A comprehensive investigation of the 500 kV DC-TL transient performance during lightning strikes is performed, taking into account different technical aspects that have not been studied in detail by previous researchers. Additionally, analysis of the back-flashover phenomenon has not been conducted well in previous work, and results on the effect of changing the lightning strike current peak and tower grounding resistance on shielding-failure flashover are quite limited. The distributed-parameter model is used to represent the DC-TL using the electromagnetic transients program (EMTP), considering real parameters of shielding wires and DC towers to study the lightning impact in the case of back-flashover and shielding-failure phenomena. Lightning strike is applied to the shielding wire, and the impact of increasing the peak value of lightning current is investigated on the back-flashover occurrence. Moreover, the influence of tower grounding resistance variation on the transient overvoltages across the tower body and back-flashover phenomenon is evaluated. From the simulation results, increasing the lightning current peak and grounding resistance results in higher overvoltages across the tower body, which increases the probability of back-flashover. Additionally, the shielding failure of the TL is assumed, and the variation impact of the lightning current peak and grounding resistance on shielding-failure flashover is investigated. The results show that the impact of the lightning current peak has a more significant impact than the grounding resistance in the case of shielding-failure flashover.

Keywords: back-flashover; DC towers; HVDC transmission; lightning strikes; lightning overvoltages; shielding failure; transient analysis

Citation: Zalhaf, A.S.; Zhao, E.; Han, Y.; Yang, P.; Almaliki, A.H.; Aly, R.M.H. Evaluation of the Transient Overvoltages of HVDC Transmission Lines Caused by Lightning Strikes. *Energies* **2022**, *15*, 1452. https://doi.org/10.3390/en15041452

Academic Editors: Tek Tjing Lie and Pawel Rozga

Received: 13 January 2022
Accepted: 14 February 2022
Published: 16 February 2022

1. Introduction

Power companies have started to pay more attention to the construction of high-voltage direct-current (HVDC) transmission systems, especially after the development of high-power electronic devices and control technologies [1,2]. Transportation of a large amount of power over long distances (≥500 km) results in problems such as reduction of power transfer, generation of reactive power and voltage profile variation [3]. Therefore, HVDC transmission is considered an optimal solution for connecting large-scale offshore renewable energy sources such as wind farms to power grids and linking distant generation sources with load centers [4,5]. Other benefits can be achieved by HVDC transmission systems, such as interconnection between unsynchronized AC systems, improving system

stability and lower transmission line costs [6,7]. As a result, HVDC applications have widely increased. In 1954, the first HVDC transmission project was constructed in Sweden [8]. Several HVDC transmission projects in China have been installed with a range of voltages starting from ±400, ±500, ±660 and ±800 kV to the forthcoming ±1100 kV to transfer electric power from large hydropower plants and wind farms over long distances [9,10]. The total transmission capacity around the world using HVDC technology is about 80 GW [11].

Most of the problems facing power grids are caused by lightning overvoltages, which result in power supply interruptions and apparatus deterioration and malfunctions. Lightning strikes are categorized into two types, direct and indirect strikes [12,13], as shown in Figure 1. Indirect strikes result in less overvoltage, which usually causes less damage to the insulator. Direct strikes, which will be the focus of this paper, are more severe than indirect strikes. Since the length of overhead DC-TLs can extend to hundreds or even thousands of kilometers, it is easy to be struck by lightning. For example, shielding wires, power conductors, towers and sometimes the nearby ground of TLs are susceptible to lightning strikes, which produce induced overvoltages. As a result, this overvoltage may result in insulator flashover, which causes a fault occurrence. When lightning strikes the shielding wire, the tower-top potential increases, which may lead to a back-flashover. On the other hand, shielding failure is when lightning strikes the power conductor directly and bypasses the shielding wire [12]. Therefore, the resulting overvoltage associated with lightning strikes must be calculated before they occur to guarantee the required electrical safety and electromagnetic compatibility level. When the overhead TL is struck by lightning, the resulting overvoltage is a function of the lightning current peak value and slope, the tower footing resistance and the tower surge impedance [14]. This resulting overvoltage propagates to nearby equipment and causes significant problems.

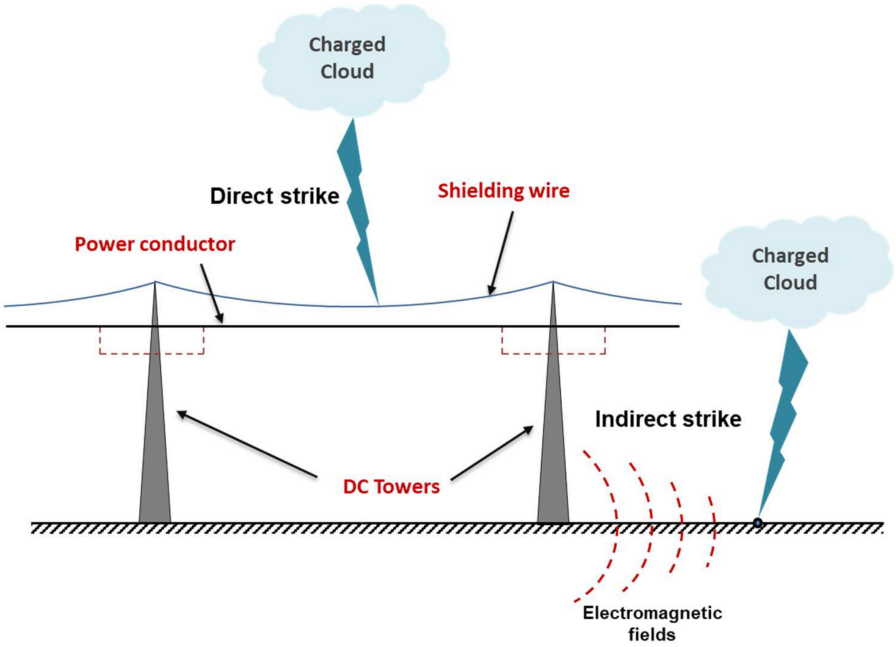

Figure 1. Schematic diagram of lightning strike mechanisms.

The influence of lightning strikes on HVDC transmission systems has been studied before [12,15–19]. A simulation model of the HVDC transmission system was presented [12] for the evaluation of lightning surge overvoltages, taking into account shielding-failure flashover and insulator back-flashover. However, the authors did not consider the influence of different peak values of lightning current on back-flashover and shielding-failure flashover. Additionally, the effect of varying the DC tower grounding resistance value on potential across the tower and back-flashover and shielding-failure flashover was not studied. The influence of modeling methods, such as selecting the lightning strike cur-

rent waveform, tower model and flashover criterion of the insulator on lightning surge overvoltages of the DC-TL, was investigated [15]. However, the authors did not study the impact of changing tower grounding resistance on transient overvoltages across the tower body and insulator back-flashover. In addition, the shielding-failure flashover case study was not taken into consideration. A simulation model using the electromagnetic transients program (EMTP) was presented [16] to study the lightning back-flashover performance of UHV-DC-TLs. The influence of changing tower footing resistance on lightning back-flashover performance was investigated. However, the influence of changing the peak value of lightning current on insulator back-flashover was not considered. Moreover, the shielding-failure flashover case study was not considered. The effect of changing the lightning current peak value on insulator flashover and varying the location of the strike along the DC-TL was analyzed [17]. However, the impact of changing the value of tower grounding resistance on transient overvoltages across the tower and insulator back-flashover and shielding-failure flashover was not investigated. Additionally, a 500 kV transmission system was simulated using PSCAD software [18] to study lightning behavior when a negative descending lightning strike terminates on the tower top. The impact of changing tower grounding resistance on the critical lightning current, which causes insulation back-flashover, was studied. However, the shielding-failure flashover case study was not investigated. Insulation back-flashover performance was studied using the 500 kV DC-TL [19]. The authors examined insulator back-flashover and calculated the lightning withstand level (critical lightning current that causes back-flashover). Additionally, they studied the variation of tower grounding resistance on insulation flashover. However, the shielding-failure flashover case study was not considered.

A summary of the literature review is given in Table 1. It could be noted that each research studied the impact of lightning strikes on DC-TLs, taking into account some technical aspects. However, back-flashover analysis has not been conducted well in the literature. In addition, shielding failure of TLs has been analyzed without investigation of important factors such as lightning current peak and tower grounding resistance. In this paper, the Yunnan-Guizhou 500 kV HVDC transmission system is used as a case study to evaluate the impact of lightning strikes, as no research investigations have been conducted to evaluate the transient behavior of DC-TLs. The 500 kV DC-TL is modeled using EMTP in the environment of ATPDraw software, including shielding wire, DC towers and span. Real system parameters and lightning current waveforms, which are widely used in power networks, are investigated to study the influence of lightning strikes on surge overvoltages in HVDC transmission systems. Hence, the impact of lightning strikes on the DC-TL can be evaluated in a realistic manner. In order to fill the gap in the literature towards better evaluation of the lightning performance of HVDC-TLs, this paper's methodology can be described in two different scenarios as follows:

1. Lightning strike is applied to the shielding wire since back-flashover analysis has not been studied well in previous studies. Then, the effect of changing the lightning current peak value is studied to check the back-flashover. Tower grounding resistance is also considered an important index for the grounding system tied to the tower body, which is a key factor for lightning protection systems. Furthermore, decreasing the value of the grounding resistance of TL towers is one of the primary solutions to reduce the back-flashover rate [12]. Therefore, the impact of varying tower grounding resistance on transient overvoltages across the tower body and back-flashover is also studied.
2. The shielding failure of the TL is studied where the strike hits the power conductor directly. The study of the influence of changing the lightning strike current peak and tower grounding resistance on shielding-failure flashover has been quite limited in previous studies. Therefore, in this case, the voltage across the insulator is calculated to check the flashover while increasing the lightning current peak. Additionally, the impact of tower grounding resistance variation on shielding-failure flashover is studied.

Table 1. Summary of the literature review.

Ref.	Considered Factors	Unconsidered Factors
[12]	• Shielding failure • Back-flashover	• Grounding resistance variation on transient overvoltages across tower, back-flashover and shielding-failure flashover • Lightning current peak change on back-flashover and shielding-failure flashover
[15]	• Back-flashover	• Grounding resistance variation on transient overvoltages across tower, back-flashover and shielding-failure flashover • Lightning current peak change on shielding-failure flashover
[16]	• Grounding resistance variation on back-flashover	• Shielding-failure flashover • Lightning current peak change on back-flashover
[17]	• Lightning current peak change on insulator flashover	• Grounding resistance variation on transient overvoltages across tower, back-flashover and shielding-failure flashover
[18]	• Grounding resistance variation on back-flashover	• Shielding-failure flashover
[19]	• Grounding resistance variation on back-flashover	• Shielding-failure flashover-

The remainder of this paper is organized as follows: The simulation model is described in detail in Section 2. Section 3 presents the characteristics of the applied lightning strike model. The simulation results are presented in Section 4. A discussion of the obtained results is introduced in Section 5, and Section 6 concludes the paper.

2. Modeling and Simulations

HVDC transmission systems consist of converters, power transformers, smoothing reactors and DC transmission lines, as shown in Figure 2. The Yunnan-Guizhou HVDC system is the world's first 500 kV three-terminal DC transmission project. This project was established to increase the consumption of hydropower in Yunnan Province and to deliver more clean energy to Guangdong Province in southeast China [20]. The distributed-parameter model of 100 km length of the DC-TL is simulated in ATPDraw, where the parameters are represented per unit length. A 2 km length from the middle of the DC-TL is divided into 4 sections, including 5 DC towers, as shown in Figure 3. Additionally, the shielding conductor, which is used to distract lightning strikes away from the poles [21], is represented in the model. Real parameters of the 500 kV DC-TL are utilized in the model, including shielding wire, DC towers and insulators.

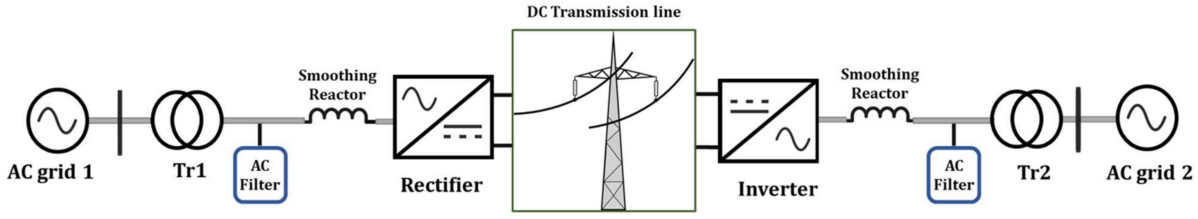

Figure 2. Configuration of HVDC transmission system.

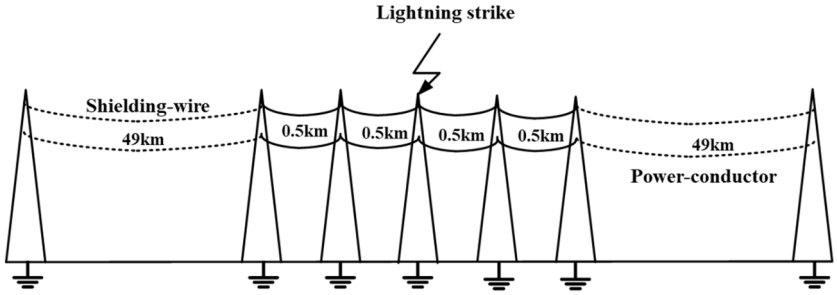

Figure 3. Model of the distributed-parameter 100 km DC transmission line.

Modeling of DC towers is essential for studying lightning overvoltages in overhead TLs. Surge propagation along the 500 kV tower structure is considered in this work by representing the vertical tower sections as single-phase constant parameter transmission lines. The impedance of these sections is calculated using the real tower structure, including the cross-arms [16,22,23].

The tower model is divided into three sections according to the geometric structure, as shown in Figure 4 [16,22,24]. Each section is divided into the tower's main body and support parts. The surge impedance (Z_{wk}) of each section, as shown in Figure 5, is calculated by using Equations (1) and (2) [16,24].

$$Z_{wk} = 60\left(ln\frac{2\sqrt{2L_k}}{r_{ek}} - 2\right), \quad k = 1,\ 2,\ 3. \tag{1}$$

$$r_{ek} = 2^{1/8}\left(r_{wk}^{1/3}r_y^{2/3}\right)^{1/4}\left(R_{wk}^{1/3}R_y^{2/3}\right)^{3/4} \tag{2}$$

where L_k, r_{wk}, r_y, R_y and R_{wk} are the lengths of corresponding parts in Figure 4.

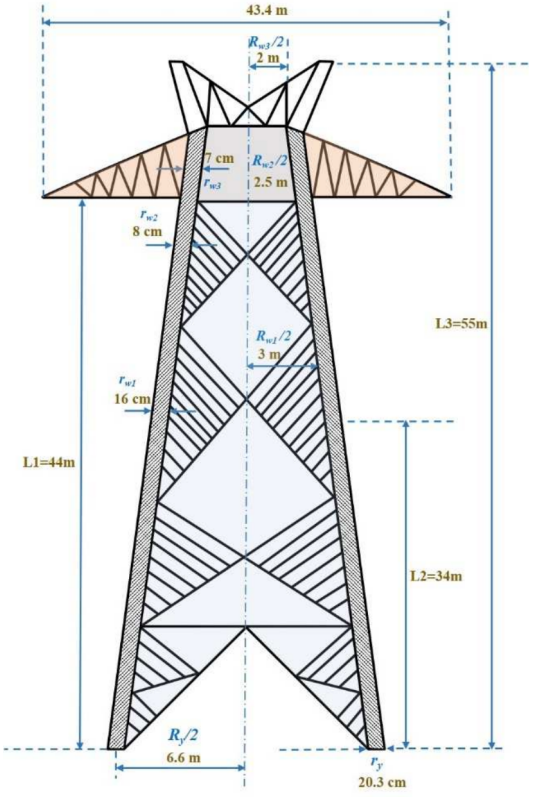

Figure 4. Geometry and dimensions of the 500 kV DC transmission tower [16].

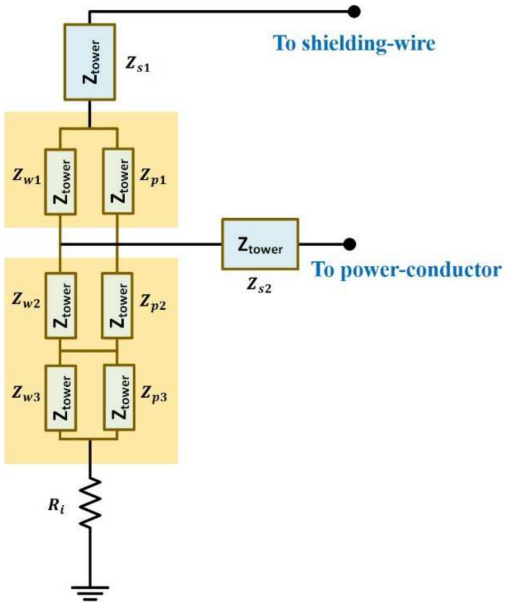

Figure 5. Surge impedance model of DC tower simulated in ATP [16].

If the influence of tower bracings is added to the main legs, the surge impedance of the conductors is reduced by about 10% [15,16,23]. Therefore, the effect of bracings is expressed by adding the surge impedance (Z_{pk}) in parallel to the main legs, as shown in Figure 5, which is calculated by Equation (3) [16,24].

$$Z_{pk} = 9Z_{wk} \tag{3}$$

The cross-arms of the DC tower are also modeled by a surge impedance (Z_{sk}), which is expressed by Equation (4), where $k = 1,\ 2$.

$$Z_{sk} = 60 \ln\left(\frac{2L_k}{r_{sk}}\right) \tag{4}$$

where L_k is the height to ground corresponding to the cross-arm of part k, and r_{sk} is the equivalent radius of the cross-arm of part k [16,24]. As shown in Figure 5, Z_{s1} is connected to the shielding wire, while Z_{s2} is connected to the power conductor.

The value of tower grounding impedance mainly affects the overvoltage values generated across the tower body. This is because tower base reflections can reach the top point of the tower faster than those from nearby towers. Hence, tower grounding impedance is calculated based on soil ionization caused by the lightning current and response time. The response time effect is usually neglected since the grounding system covers a distance less than 30 m from the tower [25]. Therefore, the current dependence is only considered while calculating tower grounding resistance (R_i), as illustrated by Equation (5) [16,26,27]:

$$R_i = \frac{R_x}{\sqrt{1 + \frac{I}{I_o}}} \tag{5}$$

where R_x is the grounding resistance of the tower at low current and low frequency, I is the current flowing through the resistance and I_o is the limiting current needed to initiate sufficient soil ionization. The grounding resistance (R_i) equals R_x when $I < I_o$ and changes according to Equation (5) when $I > I_o$. The limiting current is calculated as follows:

$$I_o = \frac{\rho_s \cdot E_o}{2\pi \cdot R_x^2} \tag{6}$$

where E_o is the soil ionization gradient (400 kV/m).

The frequency-dependent formula of soil resistivity (ρ_s) can be expressed by Equation (7), which is valid for frequency ranges from 100 Hz to 4 MHz [28]:

$$\rho_s = \rho_x \left[(f - 100)^{0.65} \cdot \left({\rho_x}^{0.73} \cdot 1.2 \times 10^{-6} \right) + 1 \right]^{-1} \quad (7)$$

where f is the frequency, and ρ_x is the resistivity of the soil at 100 Hz. In this work, the values of ρ_s and R_x are 1000 Ω·m and 10 Ω, respectively.

The equivalent circuit of the DC tower, including the impedance of each part and the grounding resistance, is shown in Figure 5.

Insulators are one of the most important components of overhead TLs. TL insulators have different types such as post, pin and string. String insulators are classified into disc, cap-pin and suspension types. The high mechanical strength, easy installation and low cost of string insulators make them widely used in overhead lines [29]. The suspension-type glass insulator string of 500 kV DC towers, with its dimensions, is shown in Figure 6a. When lightning strikes the TL, the resulting induced overvoltages may exceed the TL insulation strength resulting in a flashover. Research studies related to insulation coordination of TLs require accurate modeling of string insulator flashover to help in calculating the fast-front surges resulting from shielding-failure flashover or back-flashover of TLs. The TL insulator flashover process can be characterized using the integration method [30], volt–time curve [30,31] or by employing leader development models [32–34]. The volt–time curve, which is used in this work, is one of the most accurately used flashover criteria [15]. The insulator flash model based on the volt–time characteristics is given by Equation (8) [15,35]. Using ATPDraw, the insulator model is simulated using the flash object connected in parallel with a voltage-controlled switch, as shown in Figure 6b. Flashover happens if the voltage across the insulator string becomes equal to or higher than the flashover strength under standard lightning impulse voltages (V_{Flash}), hence the switch closes.

$$V_{Flash} = \left(400 + \frac{710}{t^{0.75}} \right) l_i \quad (8)$$

where t is the time to flashover (μs), and l_i is the insulator string length (m).

The simulation model of the DC transmission line in ATPDraw, including the power conductor, shielding wire, DC towers and insulators, is shown in Figure 7.

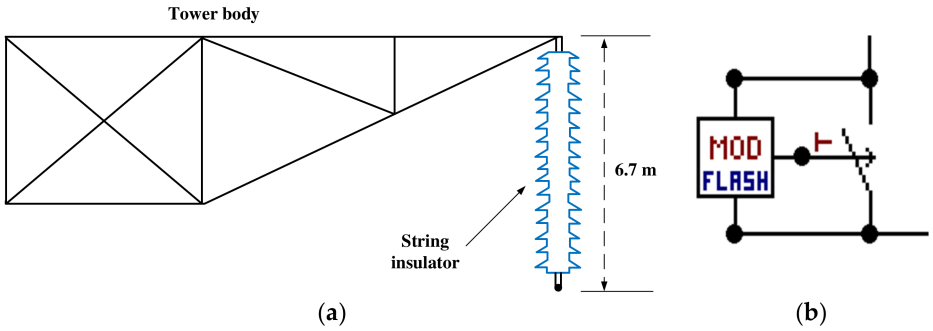

Figure 6. (**a**) Suspension-type glass insulator string of 500 kV DC-TL; (**b**) model of tower insulator string in ATPDraw.

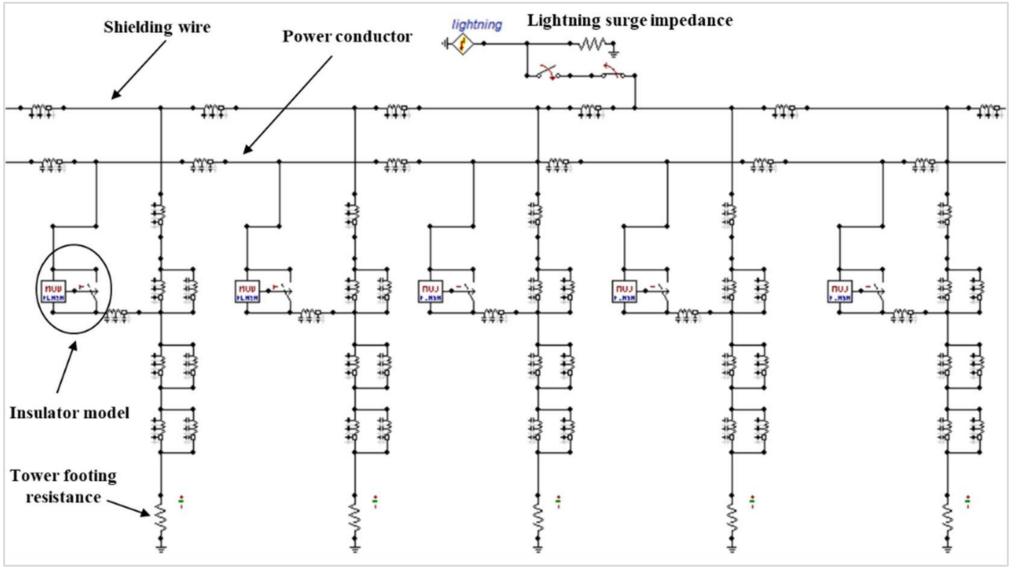

Figure 7. DC transmission line model in ATPDraw.

3. Lightning Strike Model

Lightning is considered the primary reason for unscheduled interruptions of overhead TLs in electrical networks [36]. Lightning strike is simulated in this paper by a lightning current source injected at the DC-TL to evaluate the transient overvoltages. The impedance connected in parallel with the current source is the surge impedance of the lightning channel. The estimated values of the surge impedance of the lightning channel from limited experimental and computed data range from several hundred ohms to a few kilo-ohms [31,37].

The waveshapes of the lightning strike current are represented by different numerical expressions such as double exponential [38] and Heidler functions [39]. The Heidler function is expressed by Equation (9) as follows [39,40]:

$$i(t) = I_p \cdot \frac{\left(\frac{t}{\tau_1}\right)^{\eta_{surge}}}{1 + \left(\frac{t}{\tau_1}\right)^{\eta_{surge}}} \cdot e^{\frac{-t}{\tau_2}} \quad (9)$$

where I_p is the peak value of lightning current, and η_{surge} is the shape correction coefficient. τ_1 and τ_2 are the rise time and delay time, respectively.

On the other hand, the double exponential equation, which is applied in this work, is often used to represent the strike current as follows:

$$i(t) = KI_o\left(e^{-\alpha t} - e^{-\beta t}\right) \quad (10)$$

where I_o is the lightning current peak, and K is the current peak correction factor. K, α and β are the lightning waveform data fitting constants [41].

The parameters of the standard double exponential lightning waveform 2.6/50 µs have been used in the model. The 2.6/50 µs standard waveform is usually adopted for the lightning current waveform in the design of grids lightning protection in China [42]. The values of K, I_o, α and β are 1.058, 190 kA, 0.015 μs^{-1} and 1.86 μs^{-1}, respectively [43]. The negative lightning current is used in simulations since the polarity of 75% to 90% of lightning currents is negative. The surge impedance of the lightning channel is taken as 300 Ω in the back-flashover calculations [17,42] and 800 Ω for shielding-failure calculations [44]. The injected lightning current waveform is shown in Figure 8. The values of lightning current peaks used in this work are chosen based on the real measured data suggested by the literature. For example, about 12 million samples of lightning waveforms were

detected where the largest peak current measured in various areas changes between 537 and 598 kA in the case of negative lightning waveforms and from 540 kA to 574 kA for positive lightning waveforms [45]. In another study, the measured lightning current peak was larger than 400 kA [46]. In the work presented before by Goto and Narita [47], a peak value of lightning current of 340 kA was measured in Japan. In addition, it was reported before [48,49] that the measured peak values of lightning current waveforms can reach more than 300 kA in some cases. Moreover, previous studies that discussed the lightning overvoltage and flashover phenomenon in China used high current peaks up to 490 and 358 kA such as the works presented before in [15,44], respectively. In this paper, the largest values of lightning current peaks used do not exceed 300 kA.

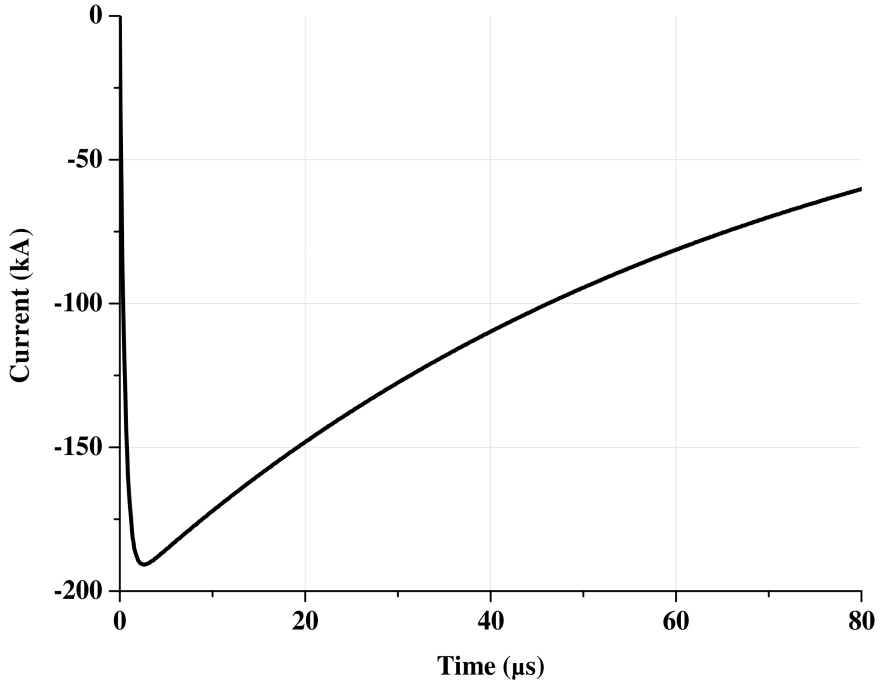

Figure 8. Injected lightning current waveform.

A flowchart summarizing the steps utilized in this paper to achieve the methodology is shown in Figure 9.

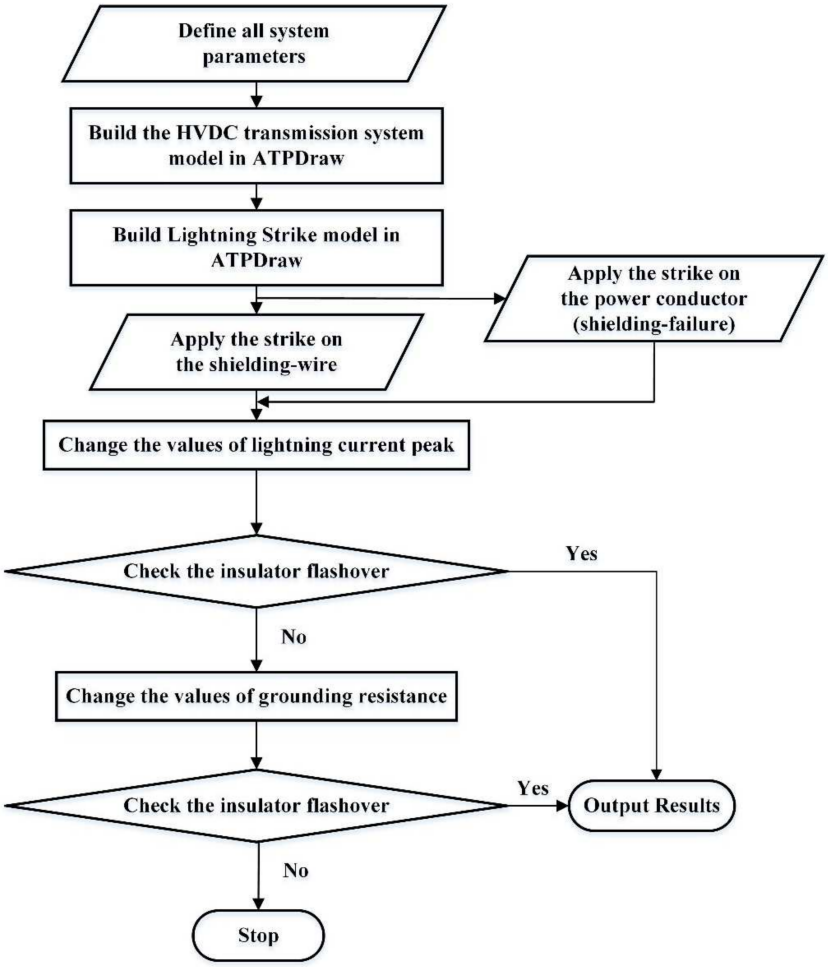

Figure 9. Flowchart describing this work's methodology.

4. Simulation Results

The simulations are carried out on the Yunnan-Guizhou 500 kV HVDC transmission system using the ATPDraw software. To verify the obtained results of the tower model, the same DC tower model, which was used before [15], is utilized in this work. A lightning current peak value (300 kA) is applied to the tower-top point at 1 µs using the standard double exponential 2.6/50 µs. The voltage across the tower insulator is calculated by subtraction of the upper voltage (power conductor) and lower voltage (tower cross-arm). Therefore, the voltage across the insulator is calculated based on the same power conductor voltage level [15] to compare the results. By calculation of the voltage across the tower insulator, it gives very close results as given before [15], as shown in Figure 10.

The impact of the lightning strike will be assessed in two scenarios. In the first scenario, the strike is injected at the shielding wire to study the back-flashover. Basically, the back-flashover risk depends on factors such as the density of ground flash (Ns, flashes/km^2/year), the peak value of lightning current and the tower footing resistance. For the back-flashover phenomenon, the annual number of lightning strikes (N_b) to a 100 km transmission line is estimated as follows [50]:

$$N_b = N_s\left(S_b + 28H^{0.6}\right)/10 \quad (11)$$

where H is the tower height (m), and S_b is the separation distance of shielding wires (m). The value of S_b equals 0 for a single shielding wire.

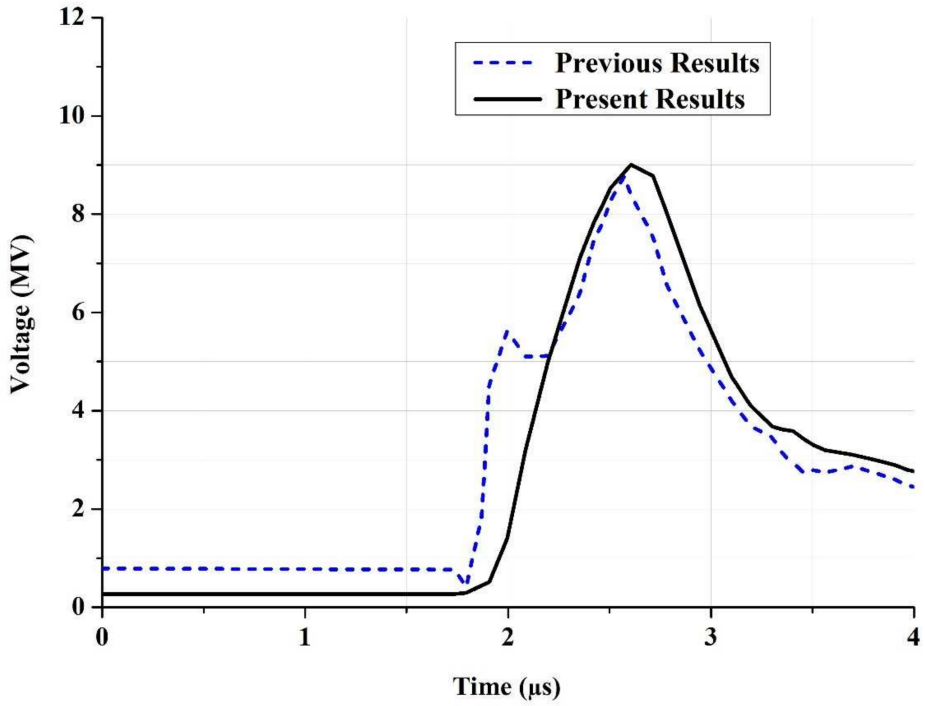

Figure 10. Comparison between the voltage across insulator in the present and previous results [15] while applying the strike at tower top using the same tower model.

In this case, the influence of changing lightning current peak value on the insulator back-flashover is assessed. In the same case, the impact of changing the tower grounding resistance on the transient overvoltages across the tower is investigated. Additionally, the back-flashover probability is checked by increasing the tower grounding resistance.

In the second scenario, the lightning strike hits the power conductor directly (shielding failure). Then, the impact of changing the position of the strike along the power conductor is investigated. Moreover, the influence of increasing the lightning current peak and tower grounding resistance on the insulation flashover is investigated.

4.1. Applying the Lightning Strike on the Shielding Wire

In this case, the shielding wire is struck by lightning, and the lightning current peak value is changed from 10 kA to 190 kA at 10 Ω grounding resistance, as illustrated by Figures 11–15. At each current peak value, the insulator's lowest point (tower cross-arm point) voltage and voltage at the insulator highest point (which lies on the power conductor) are measured to check the back-flashover. If there is no flashover on the insulator, the power conductor voltage remains 500 kV after applying the lightning. If the insulator has a flashover after applying the lightning strike, the voltage of the power conductor goes to zero, which means that the TL exhibits a back-flashover. As shown in Figures 11 and 12, the current peak is set to 10 kA and 28 kA, respectively.

When lightning strike is applied, the traveling wave of the tower cross-arm voltage varies alternatively and declines to zero after some refractions and reflections since there is no flashover. Additionally, it can be noted that the voltage of the power conductor remains at 500 kV after applying the strike, which means that there is no flashover, and the strike current is discharged to the earth. On the other hand, when the current peak magnitude is increased to 50 kA, 100 kA and 190 kA, as illustrated in Figures 13–15, respectively, the power conductor voltage decreases to zero after applying the strike. This means that there is a flashover across the insulator, and the TL has a back-flashover. The flashover occurred since the voltage across the insulator is larger than the insulator withstand voltage; hence, the voltage-controlled switch closed.

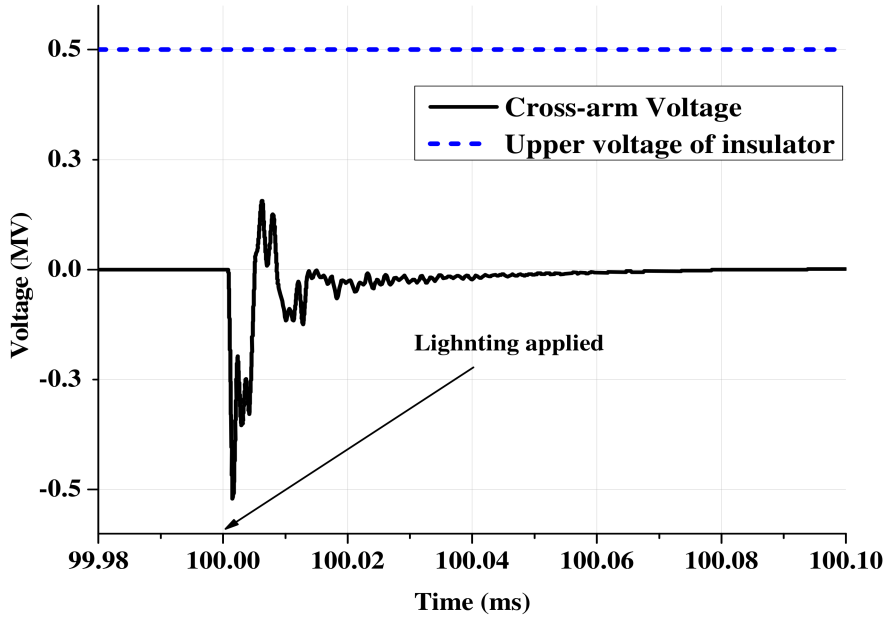

Figure 11. Voltage at tower cross-arm point and upper point of insulator with 10 kA lightning current.

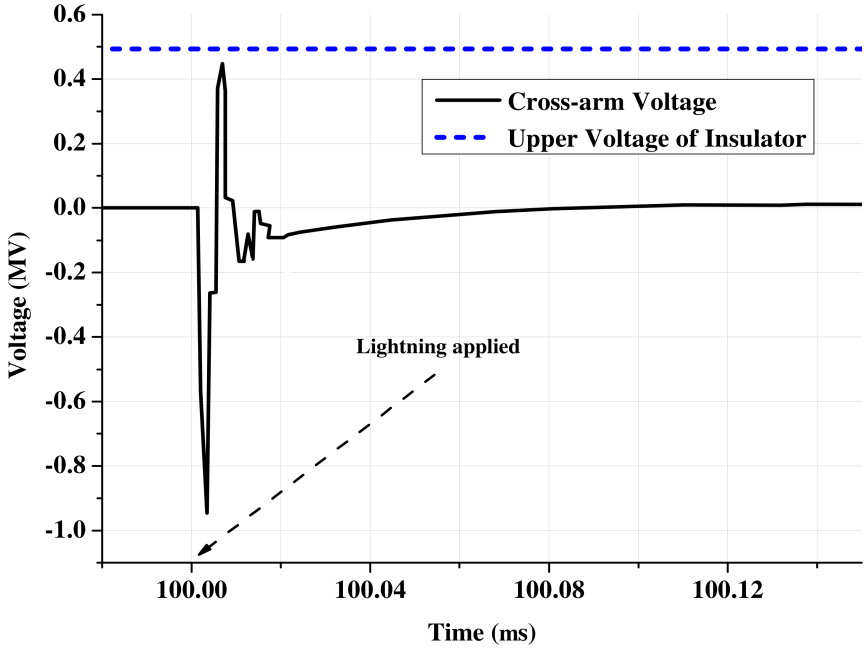

Figure 12. Voltage at tower cross-arm point and upper point of insulator with 28 kA lightning current.

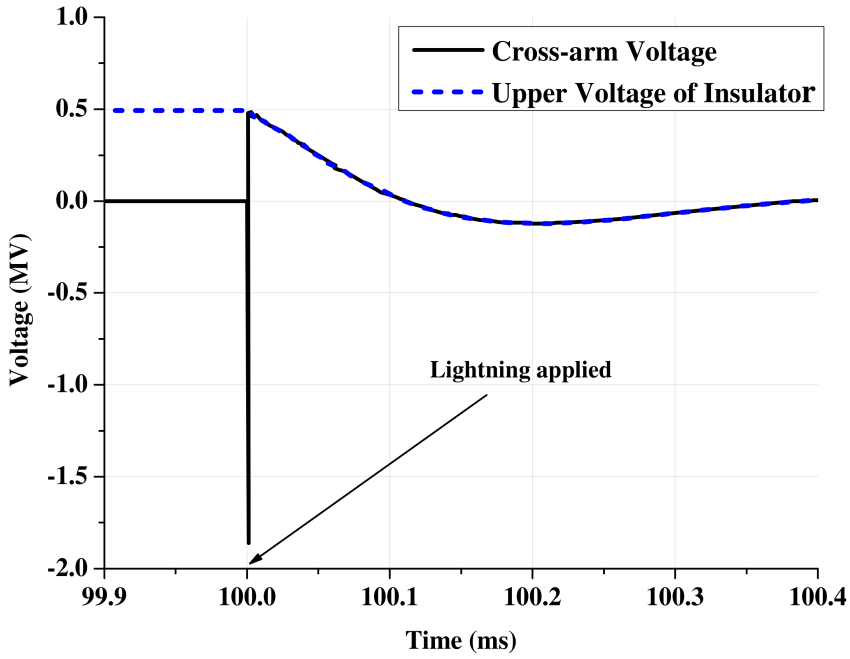

Figure 13. Voltage at tower cross-arm point and upper point of insulator with 50 kA lightning current.

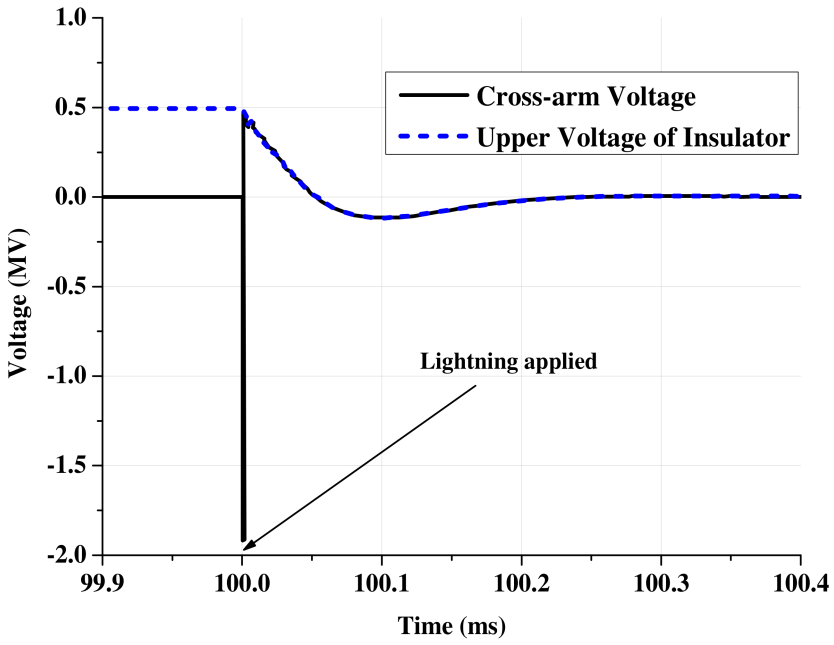

Figure 14. Voltage at tower cross-arm point and upper point of insulator with 100 kA lightning current.

Moreover, the influence of changing the tower grounding resistance is studied on the transient overvoltages across the tower. The tower grounding resistance has been changed from 5 Ω to 20 Ω, and the temporal variation of voltage has been calculated at the tower top and tower cross-arm, as illustrated in Figures 16 and 17, respectively. The two figures show that the overvoltage values at different points along the tower increase with the increase in the grounding resistance value. Additionally, the grounding resistance value has been increased to 50 Ω and 125 Ω to see the impact on the insulator flashover, with a lightning current peak value equal to 28 kA, as shown in Figures 18 and 19, respectively. As shown in Figure 18, with a ground resistance value equal to 50 Ω, no flashover occurs, while in Figure 19, the insulator has a flashover, which confirms that the increasing the grounding

resistance is a primary reason for insulation back-flashover. Hence, the grounding resistance has a significant role in the overvoltage variation across the tower body, which increases the probability of back-flashover.

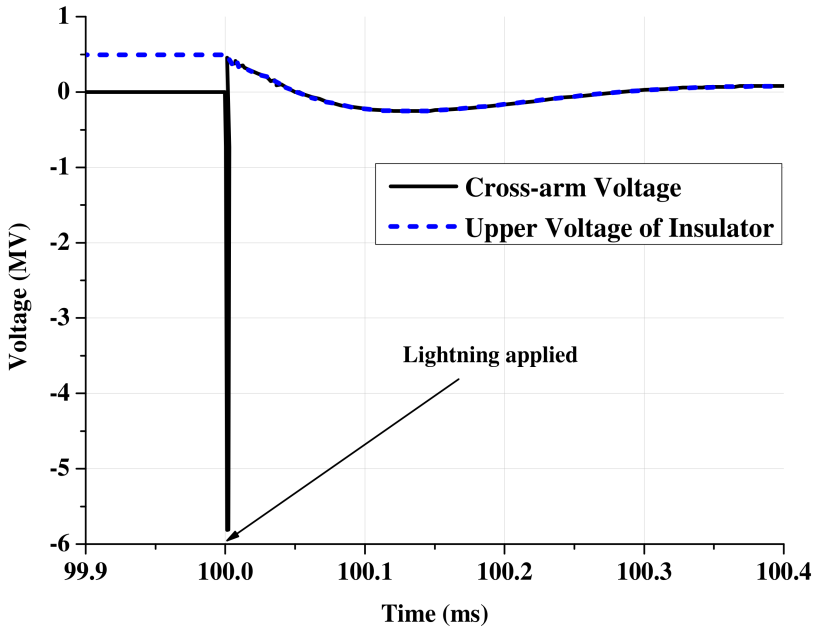

Figure 15. Voltage at tower cross-arm point and upper point of insulator with 190 kA lightning current.

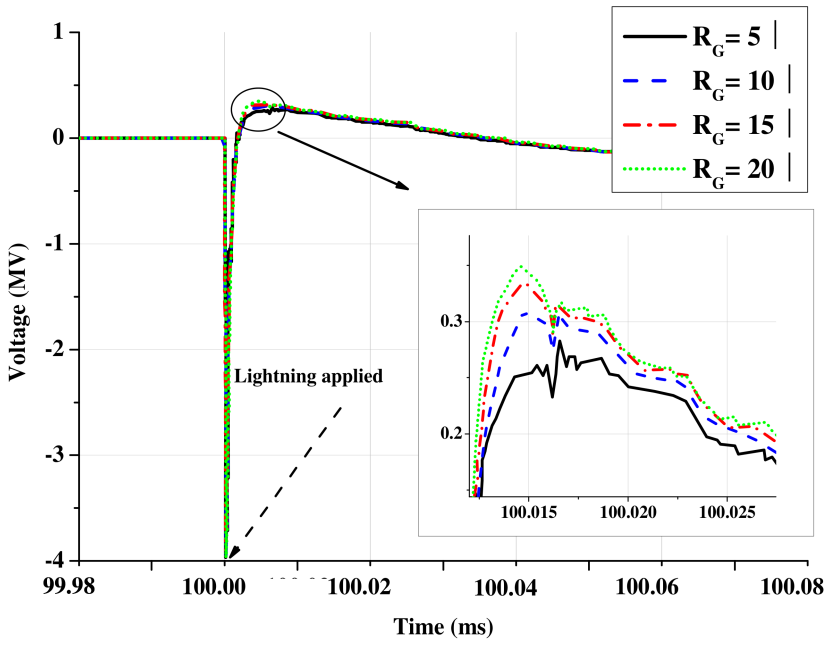

Figure 16. Voltage of the shielding wire at the strike point with changing tower grounding resistance.

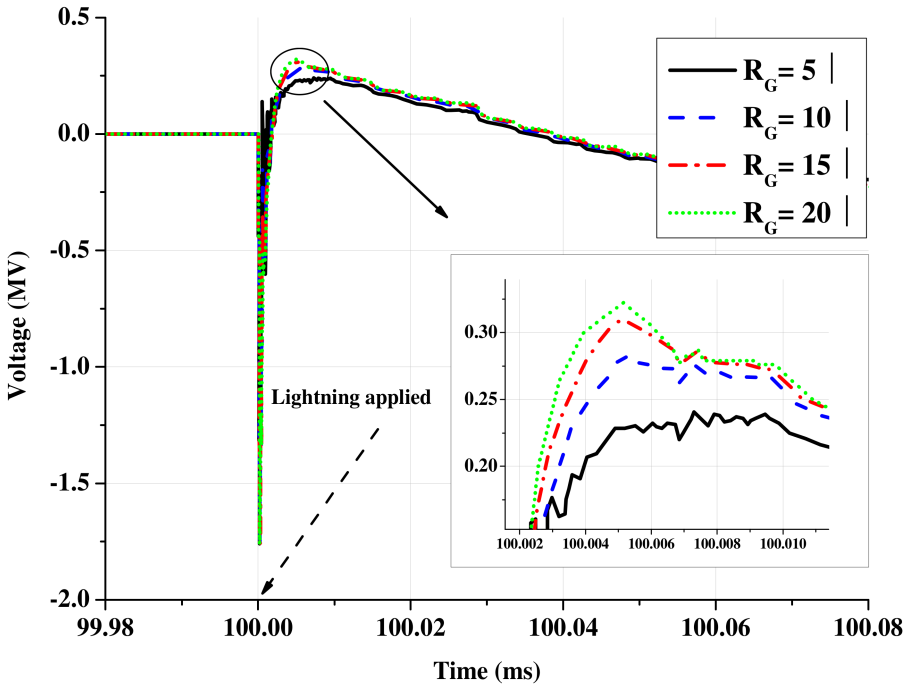

Figure 17. Voltage at DC tower cross-arm with changing tower grounding resistance.

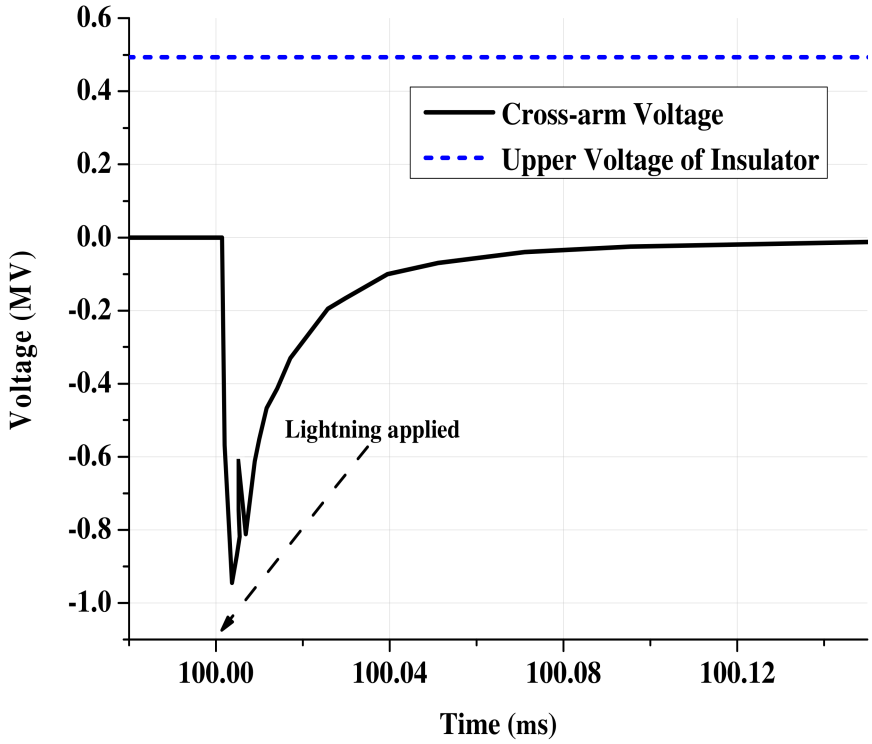

Figure 18. Voltage at tower cross-arm point and upper point of insulator at 28 kA and 50 Ω grounding resistance.

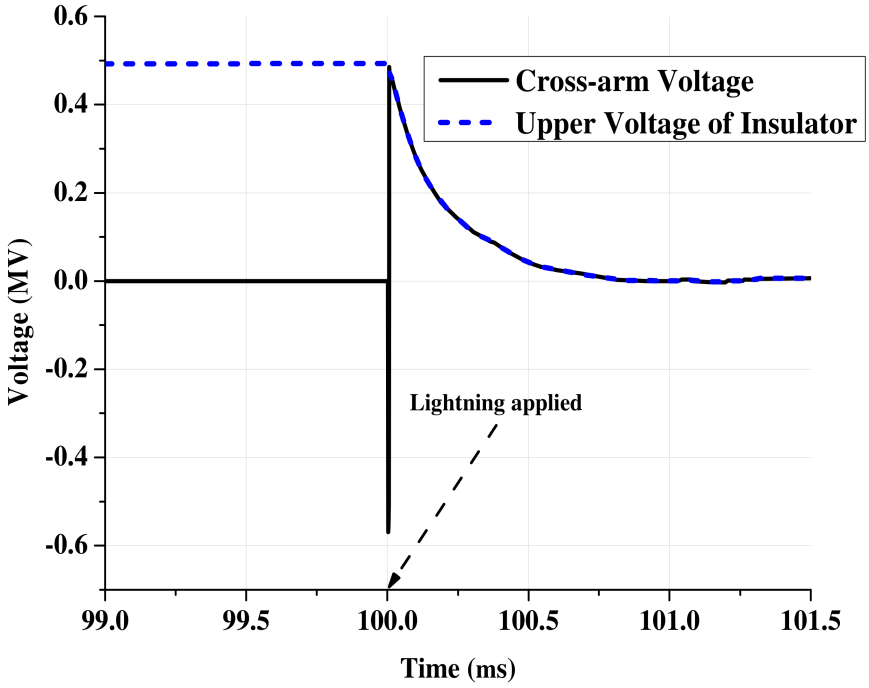

Figure 19. Voltage at tower cross-arm point and upper point of insulator at 28 kA and 125 Ω grounding resistance.

4.2. Applying the Lightning Strike on the Transmission Line (A Shielding Failure)

In this part, the voltage across the insulator has been measured to check the flashover by changing the lightning current peak value. At higher transmission voltages levels, it is not necessary that the flashover occurs in the case of shielding failure with low values of lightning current. Hence, the critical or minimum current value (I_{SF}) required to induce a flashover is expressed as follows [51]:

$$I_{SF} = 2CFO/Z_{Surge} \quad (12)$$

where CFO is the critical lightning impulse flashover voltage, and Z_{Surge} is the surge impedance of the conductor under corona.

The strike is applied at the midpoint of the power conductor where the lightning current peak is set to 100 kA and 300 kA, as shown in Figures 20 and 21, respectively. The voltages at the upper point of the insulator (which lies on the power conductor) and tower cross-arm point are measured. It can be noted that no flashover occurs at 100 kA since the insulator upper point voltage returns to 500 kV after applying the strike, as shown in Figure 20. Additionally, the cross-arm voltage remains zero after the strike injection. On the other hand, as shown in Figure 21, the voltage of the insulator upper point declined to zero after applying the strike, which means that the insulator has a flashover. Since the voltage across the insulator was greater than the critical flashover voltage, the voltage-controlled switch closed, and the insulator upper point voltage declined to zero. Additionally, the tower grounding resistance was varied at 100 kA to check its influence on the shielding-failure flashover. By changing the grounding resistance value from 10 Ω to 1000 Ω, it gives a very close behavior to Figure 20, and there is no flashover. Hence, shielding-failure flashover is influenced primarily by lightning current peak variation, while the impact of grounding resistance variation can be disregarded.

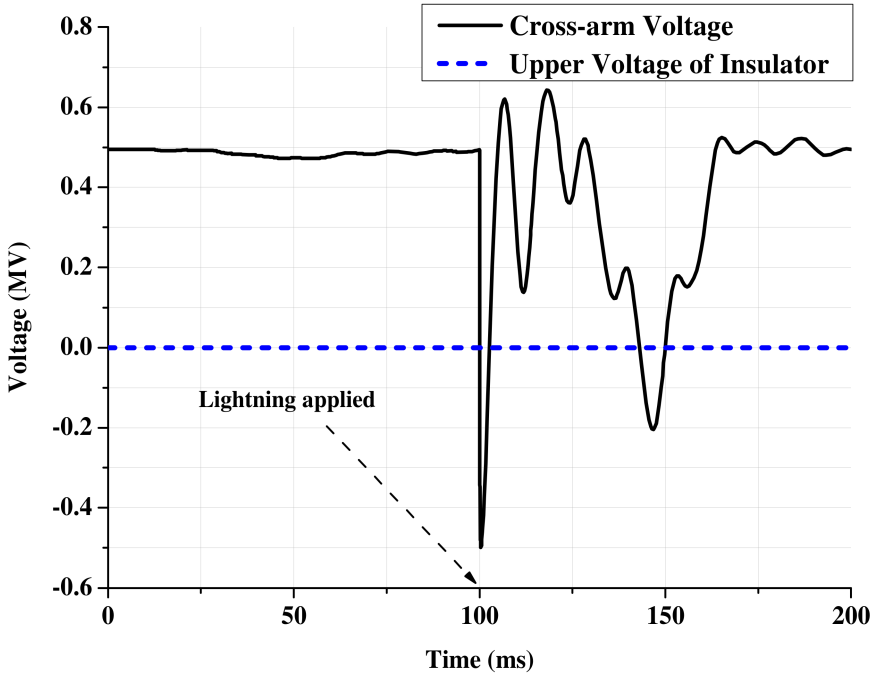

Figure 20. Voltage at tower cross-arm point and upper point of insulator in the case of shielding failure at 100 kA.

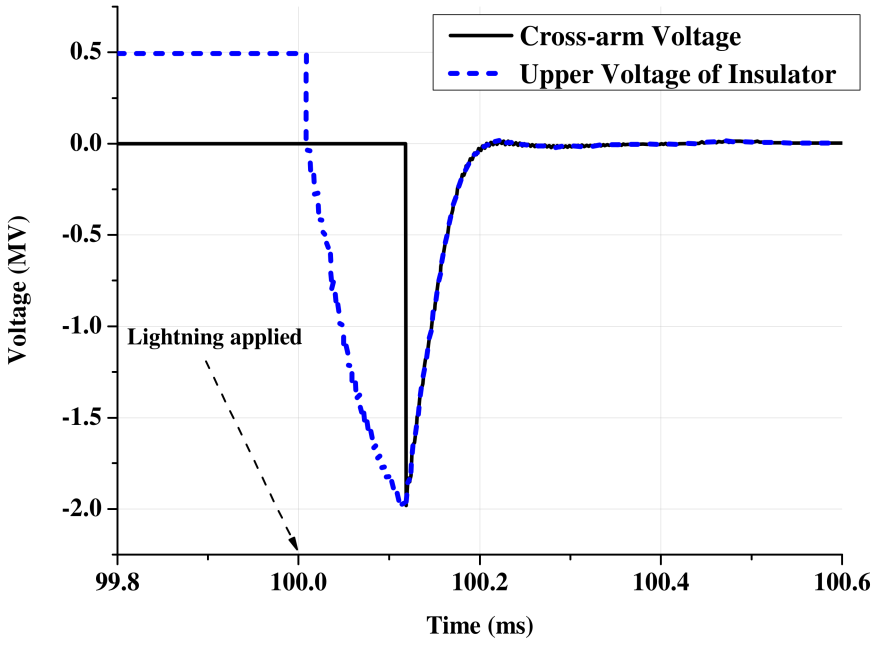

Figure 21. Voltage at tower cross-arm point and upper point of insulator in the case of shielding failure at 300 kA.

5. Discussion of Obtained Results

The same tower model used before [15] has been employed in this paper to validate the obtained results. To verify the obtained results, the voltage across the tower insulator has been compared with its counterpart given before in the literature. By applying the same standard lightning waveform (2.6/50 μs) with the same current peak at the same voltage level, the results are matching well. By increasing the lightning current peak value (>28 kA), the back-flashover occurred since the insulator could not withstand the voltage created. Additionally, the transient overvoltage across the tower increases with the rise

of the grounding resistance value, which resulted in a back-flashover occurrence (with grounding resistance >100 Ω). Therefore, the DC tower should be tied to the grounding system with a smaller resistance to limit the increase in the induced overvoltage values, which may lead to insulation back-flashover. This confirms that the proper design of the grounding system under the tower, which ensures smaller grounding resistance is essential for the protection of HVDC transmission systems from lightning strike hazards. This will help in the appropriate sizing of lightning protective devices to avoid harmful damage to towers and to ensure the safety of personnel.

In addition, a shielding failure case study is assumed, where the strike hits the power conductor directly. By increasing the lightning current peak value ($\geq$300 kA), the tower insulator has a flashover since it could not withstand the voltage applied during the shielding failure. Additionally, by changing the grounding resistance value up to 1000 Ω, there is no flashover occurred. This confirms that the impact of lightning current peak variation has a more significant impact than the grounding resistance variation on insulator flashover, which can be ignored in the case of shielding failure. On the other hand, the back-flashover of the DC-TLs is affected considerably by the lightning current peak value and tower grounding resistance.

6. Conclusions

In this study, the influence of lightning strike overvoltages on the DC-TL of the Yunnan-Guizhou 500 kV HVDC transmission system has been assessed, as no research investigations have been conducted to study the lightning transient behavior in this system. Additionally, back-flashover analysis has not been conducted well in the literature. Moreover, important factors such as the effect of changing lightning current peak and tower grounding resistance on the transient overvoltages have not been considered during the shielding failure in previous works. Hence, the main conclusions that can be extracted from this work are summarized as follows:

(1) The probability of insulation back-flashover increases with the increase in the lightning current peak and tower grounding resistance.
(2) Choosing the proper parameters of the grounding system under the DC tower is essential for the lightning protection system design.
(3) In the case of the shielding failure of DC-TL, with the increase of the lightning current peak value, the possibility of insulator flashover increases.
(4) In contrast, the grounding resistance change has an insignificant impact on insulator flashover in the case of shielding failure.
(5) The study offers a research platform for the identification of back-flashover and shielding-failure phenomena and enables the straightforward evaluation of the lightning performance of the HVDC transmission systems.

There are some extensions to be investigated in relation to the present work, such as evaluating the surge impedance value of DC towers when using multiple shielding wires in parallel, connected from the top of the tower to the tower footing. This arrangement can help in decreasing the surge impedance of the tower where more current pathways can be provided using multiple shielding wires; hence, the flashover phenomenon can be mitigated. In addition, the study can be extended to include the influence of lightning strikes on renewable energy sources such as wind turbines and photovoltaic systems.

Author Contributions: Conceptualization, methodology and original draft preparation, A.S.Z., E.Z. and Y.H.; reviewing and editing, P.Y.; reviewing, editing and funding acquisition, A.H.A. and R.M.H.A. All authors have read and agreed to the published version of the manuscript.

Funding: This research was funded by Taif University, Researchers Supporting Project grant number (TURSP-2020/252).

Institutional Review Board Statement: Not applicable.

Informed Consent Statement: Not applicable.

Data Availability Statement: Not applicable.

Acknowledgments: The author would like to acknowledge the financial support provided by Taif University Researchers Supporting Project Number (TURSP-2020/252).

Conflicts of Interest: The authors declare no conflict of interest.

References

1. Merlin, M.C.; Green, T.C.; Mitcheson, P.D.; Trainer, D.R.; Critchley, R.; Crookes, W. The alternate arm converter: A new hybrid multilevel converter with DC-fault blocking capability. *IEEE Trans. Power Deliv.* **2014**, *29*, 310–317. [CrossRef]
2. Barnes, M.; Van Hertem, D.; Teeuwsen, S.P.; Callavik, M. HVDC Systems in Smart Grids. *Proc. IEEE* **2017**, *105*, 2082–2098. [CrossRef]
3. Kamakshaiah, S.; Kamaraju, V. *HVDC Transmission*; McGraw-Hill Education: New York, NY, USA, 2011; ISBN 9789353161033.
4. Christodoulou, C.; Lazarou, S.; Zafiropoulos, E.; Vita, V.; Ekonomou, L. HV multi-terminal DC lines as the backbone of the energy transmission system—A research plan to tackle challenges. *MATEC Web Conf.* **2019**, *292*, 01067. [CrossRef]
5. Lekić, A.; Hermans, B.; Jovičić, N.; Patrinos, P. Microsecond nonlinear model predictive control for DC-DC converters. *Int. J. Circuit Theory Appl.* **2020**, *48*, 406–419. [CrossRef]
6. Hu, J.; Wang, J.; Xiong, X.; Chen, J. A Post-Contingency Power Flow Control Strategy for AC/DC Hybrid Power Grid Considering the Dynamic Electrothermal Effects of Transmission Lines. *IEEE Access* **2019**, *7*, 65288–65302. [CrossRef]
7. Nguyen, T.V.; Petit, P.; Aillerie, M.; Salame, C.; Charles, J.-P. Efficiency of magnetic coupled boost DC-DC converters mainly dedicated to renewable energy systems: Influence of the coupling factor. *Int. J. Circuit Theory Appl.* **2015**, *43*, 1042–1062. [CrossRef]
8. Li, T. General. In *UHV Transmission Technology*, 1st ed.; The China Electric Power Research; Elsevier: Amsterdam, The Netherlands, 2018; pp. 387–399; ISBN 9780128051931.
9. Hu, B.; Xie, K.; Tai, H.M. Optimal Reliability Allocation of ±800 kV Ultra HVDC Transmission Systems. *IEEE Trans. Power Deliv.* **2018**, *33*, 1174–1184. [CrossRef]
10. Zhao, L.; Cui, X.; Xie, L.; Lu, J.; He, K.; Ju, Y. Altitude Correction of Radio Interference of HVDC Transmission Lines Part II: Measured Data Analysis and Altitude Correction. *IEEE Trans. Electromagn. Compat.* **2017**, *59*, 284–292. [CrossRef]
11. Fu, Z.; Sima, W.; Yang, M.; Sun, P.; Tao, Y. A Mutual-inductance-type Fault Current Limiter in MMC-HVDC Systems. *IEEE Trans. Power Deliv.* **2020**, *35*, 2403–2413. [CrossRef]
12. Shu, H.C.; Zhang, G.B.; Zhu, Z.Z.; Zhu, S.Q. Modeling and simulation of lightning electromagnetic transient and identification of shielding failure and back striking in ±800kV UHVDC transmission lines: Part I: Modeling and simulation of lightning electromagnetic transient. In Proceedings of the Asia-Pacific Power and Energy Engineering Conference, APPEEC, IEEE, Wuhan, China, 27–31 March 2009; pp. 1–4.
13. Ahmadi, M.E.; Niasati, M.; Barzegar-Bafrooei, M.R. Enhancing the lightning performance of overhead transmission lines with optimal EGLA and downstream shield wire placement in mountainous areas: A complete study. *IET Sci. Meas. Technol.* **2020**, *14*, 564–575. [CrossRef]
14. Christodoulou, C.A.; Vita, V.; Voglitsis, D.; Milushev, G.; Ekonomou, L. A Heuristic method for the reduction of the outage rate of high-voltage substations due to atmospheric overvoltages. *Appl. Sci.* **2018**, *8*, 273. [CrossRef]
15. Han, Y.; Li, L.; Chen, H.; Lu, Y. Influence of Modeling Methods on the Calculated Lightning Surge Overvoltages at a UHVDC Converter Station Due to Backflashover. *IEEE Trans. Power Deliv.* **2012**, *27*, 1090–1095. [CrossRef]
16. Qing, Y.; Jie, H.A.O.; Jie, E.N.G.; Labo, K.; Uni, C. Lightning Back-Flashover Performance of the Yun-Guang UHV DC Transmission Lines. *High Volt. Eng.* **2008**, *34*, 1330–1335.
17. Xing, L.; Weng, H.; Wang, L.; Ma, L.; Wu, C.; Wang, X. Transient simulation of lightning strokes on HVDC transmission lines and fault pole selection. In Proceedings of the 2017 2nd International Conference on Power and Renewable Energy, ICPRE 2017, Chengdu, China, 20–23 September 2017; pp. 219–224. [CrossRef]
18. Liu, P.; Wu, G.N.; Sui, B.; Li, R.F.; Cao, X.B. Modeling lightning performance of transmission systems using PSCAD. In Proceedings of the 2008 International Conference on High Voltage Engineering and Application, ICHVE 2008, Chongqing, China, 9–12 November 2008; pp. 168–171.
19. Yilin, W.; Fan, W.; Zhi, L.; Tai, W. Research on lightning protection performance of HVDC ± 500 kV transmission lines based on Bergeron algorithm WANG. *Heilongjiang Electr. Power* **2015**, *37*, 228–231.
20. China Southern Power Grid. Available online: http://eng.csg.cn/Press_release/News_2020/202006/t20200630_312010.html (accessed on 2 August 2021).
21. IEEE Transmission and Distribution Committee; High Voltage Direct Current Working Group. *Guide for High Voltage Direct Current Overhead Transmission Line Design*; IEEE: New York, NY, USA, 2018.
22. Yamada, T.; Mochizuki, A.; Sawada, J.; Zaima, E.; Kawamura, T.; Ametani, A.; Ishii, M.; Kato, S. Experimental evaluation of a UHV tower model for lightning surge analysis. *IEEE Trans. Power Deliv.* **1995**, *10*, 393–402. [CrossRef]
23. Hara, T.; Yamamoto, O. Modelling of a transmission tower for lightning-surge analysis. *IEE Proc. Gener. Transm. Distrib.* **1996**, *143*, 283–289. [CrossRef]
24. Martinez-Velasco, J.A. *Power System Transients: Parameter Determination*; CRC Press, Taylor & Francis Group: New York, NY, USA, 2010; ISBN 9781420065299.

25. Imece, A.F.; Durbak, D.W. Modeling guidelines for fast front transients. *IEEE Power Eng. Rev.* **1996**, *16*, 67.
26. Mesic, M.; Uglsic, I.; Grcic, B.F.; Piliskic, S.; Mi, M.; Franc, B. Overvoltage Protection Performance of the 110 kV Overhead Lines after the Line Surge Arresters Implementation. In Proceedings of the International Conference on Power Systems Transients (IPST2015), Cavtat, Croatia, 15–18 June 2015; pp. 1–7.
27. *IEC/TR 60071-4*; Insulation Co-Ordination—Part 4: Computational Guide to Insulation Co-Ordination and Modelling of Electrical Networks. IEC: Geneva, Switzerland, 2004.
28. Alipio, R.; Visacro, S. Impulse efficiency of grounding electrodes: Effect of frequency-dependent soil parameters. *IEEE Trans. Power Deliv.* **2014**, *29*, 716–723. [CrossRef]
29. Izgi, E.; Inan, A.; Ay, S. The analysis and simulation of voltage distribution over string insulators using matlab/simulink. *Electr. Power Compon. Syst.* **2008**, *36*, 109–123. [CrossRef]
30. Darveniza, M.; Vlastos, A.E. The Generalized Integration Method for Predicting Impulse Volt-Time Characteristics for non-Standard Wave Shapes—A Theoretical Basis. *IEEE Trans. Electr. Insul.* **1988**, *23*, 373–381. [CrossRef]
31. Datsios, Z.G.; Mikropoulos, P.N.; Tsovilis, T.E. Effects of Lightning Channel Equivalent Impedance on Lightning Performance of Overhead Transmission Lines. *IEEE Trans. Electromagn. Compat.* **2019**, *61*, 623–630. [CrossRef]
32. *CIGRE WG01 SC33*; Guide to Procedures for Estimating the Lightning Performance of Transmission Lines. CIGRE: Paris, France, 1991; Volume 1.
33. Motoyama, H. Experimental study and analysis of breakdown characteristics of long air gaps with short tail lightning impulse. *IEEE Trans. Power Deliv.* **1996**, *11*, 972–979. [CrossRef]
34. Mozumi, T.; Baba, Y.; Ishii, M.; Nagaoka, N.; Ametani, A. Numerical Electromagnetic Field Analysis of Arc-Horn Voltages during a Back-Flashover on a 500 KV Twin-Circuit Line. *IEEE Power Eng. Rev.* **2002**, *22*, 72. [CrossRef]
35. Datsios, Z.G.; Mikropoulos, P.N.; Tsovilis, T.E. Insulator string flashover modeling with the aid of an ATPDraw object. In Proceedings of the Universities Power Engineering Conference, Soest, Germany, 5–8 September 2011; pp. 1–5.
36. Nayel, M. Analysis of lightning-attractive areas around high-voltage direct current transmission line. *Electr. Power Compon. Syst.* **2009**, *37*, 146–157. [CrossRef]
37. Wang, Y.; Zhang, X.; Tao, S. Modeling of Lightning Transients in Photovoltaic Bracket Systems. *IEEE Access* **2019**, *7*, 12262–12271. [CrossRef]
38. Jia, W.; Xiaoqing, Z. Double-Exponential Expression of Lightning Current Waveforms. In Proceedings of the 2006 4th Asia-Pacific Conference on Environmental Electromagnetics, IEEE, Dalian, China, 1–4 August 2006; pp. 320–323.
39. Heidler, F.; Cvetic, J.M.; Stanic, B.V. Calculation of lightning current parameters. *IEEE Trans. Power Deliv.* **1999**, *14*, 399–404. [CrossRef]
40. *IEC 62305-3*; Protection against Lightning Part 3: Physical Damage to Structures and Life Hazard. IEC: Geneva, Switzerland, 2010; p. 313.
41. Fang, S.; Zhang, L.; Zou, L.; Chen, Y.; Wang, Y. Study on lightning overvoltage and commutation failure in UHV AC/DC hybrid system. *J. Eng.* **2019**, *2019*, 2677–2682. [CrossRef]
42. Zhou, H.; Qiu, W.; Sun, K.; Chen, J.; Deng, X.; Qian, F.; Wang, D.; Zhao, B.; Li, J.; Li, S.; et al. (Eds.) *Ultra-High Voltage AC/DC Power Transmission*, 1st ed.; Springer: Berlin/Heidelberg, Germany, 2018; ISBN 9783662545737.
43. Xiaohui, W.; Zhang, X.; Dasheng, Y. An efficient algorithm of transient responses on wind turbine towers struck by lightning. *Int. J. Comput. Math. Electr. Electron. Eng. COMPEL* **2009**, *28*, 372–384. [CrossRef]
44. Han, Y.; Tang, L.; Li, L.; He, Q.; Hao, Y.; Yao, S. Influence of lightning flashover criterion on the calculated lightning withstand level of ±800 kV UHVDC transmission lines at high altitude. *IEEE Trans. Dielectr. Electr. Insul.* **2015**, *22*, 185–191. [CrossRef]
45. Kochtubajda, B.; Burrows, W.R.; Power, B.E. Large current lightning flashes in Canada: 1999–2006. In Proceedings of the 20th International Lightning Detection Conference, Tucson, AZ, USA, 21–23 April 2008; pp. 1–6.
46. Lyons, W.A.; Uliasz, M.; Nelson, T.E. Large peak current cloud-to-ground lightning flashes during the summer months in the contiguous United States. *Mon. Weather. Rev.* **1998**, *126*, 2217–2233. [CrossRef]
47. Goto, Y.; Narita, K. Electrical characteristics of winter lightning. *J. Atmos. Terr. Phys.* **1995**, *57*, 449–458. [CrossRef]
48. *CIGRE WG C4.407*; Lightning Parameters for Engineering Applications. IEEE: New York, NY, USA, 2013.
49. Cooray, V.; Rakov, V. On the upper and lower limits of peak current of first return strokes in negative lightning flashes. *Atmos. Res.* **2012**, *117*, 12–17. [CrossRef]
50. Lennerhag, O.; Lundquist, J.; Engelbrecht, C.; Karmokar, T.; Bollen, M.H.J. An Improved Statistical Method for Calculating Lightning Overvoltages in HVDC Overhead Line/Cable Systems. *Energies* **2019**, *12*, 3121. [CrossRef]
51. Grzybowski, S.; Hileman, R.; Longo, J.; Moser, H. Estimating lightning performance of transmission lines. II. Updates to analytical models. *IEEE Trans. Power Deliv.* **1993**, *8*, 1254–1267. [CrossRef]